UAL/ETEAPOT Results for Proton EDM Benchmark Lattices

J. D. Talman and R. M. Talman

April 27, 2012

Abstract

The three benchmark lattices for an all-electric proton EDM ring are investigated using UAL/ETEAPOT. They have field indices $m = -1$, $m \approx 0$, and $m = 1$. Values of horizontal and vertical tunes, and beta functions at the origin (midway between adjacent bends) are tabulated. Results are compared to values obtained from a linearized transfer matrix formalism. In all cases the design vertical tunes have been adjusted to Q_y=0.2.

1 Introduction

All-electric lattices for a storage ring to measure the electric dipole moment (EDM) of the proton are described in the BNL proposal by the Storage Ring EDM Collaboration, *A Proposal to Measure the Proton Electric Dipole Moment with* 10^{-29} *e-cm Sensitivity*[1]. The present report provides lattices stripped down to their bare essentials in order to simplify benchmark comparisons of various simulation codes.

An electric field with index m power law dependence on radius r for y=0 is

$$\mathbf{E}(r,0) = -E_0 \, \frac{r_0^{1+m}}{r^{1+m}} \, \hat{\mathbf{r}}, \tag{1}$$

and the electric potential $V(r)$, adjusted to vanish at $r = r_0$, is

$$V(r) = -\frac{E_0 r_0}{m} \left(\frac{r_0^m}{r^m} - 1 \right). \tag{2}$$

The "cleanest" case theoretically has m=1, in which case it is known as the Kepler or the Coulomb electric field. Our problem is a bit more general than this terminology suggests, since our treatment is necessarily relativistic. For m=1 the Kepler problem can be solved with the same generality in the relativistic as in the nonrelativistic case; the orbits are no longer exactly elliptical, nor exactly closed however[3].

The full ring is circular and consists of 40 identical cells. A single cell is shown in Figure 1. With curved planar plates, which is the easiest configuration to build, the field boundaries are concentric cylinders and the field index is m=0. The optimal (i.e. longest) spin coherence time (SCT) is expected to be close to this value. For m=1 the field boundaries are concentric spheres.

For m=0 the fields are independent of vertical displacement y so there is no vertical focusing. Vertical stability requires focusing quadrupoles, labeled q in Figure 1. Even if not required for vertical stability the q quadrupoles are necessary for adjusting the vertical tune Q_y of the storage ring. The vertical tunes have been adjusted to $Q_y = 0.2$ for all three of the benchmark lattices described in the next section.

2 Parameters of Benchmark Lattices

Analytic, linearized transfer matrix MAPLE programs with names `E_BM_P1.0.mw` `E_BM_Z.mw`, and `E_BM_M1.0.mw` are in `/home/talman/EDM/EDM-lattice/maple/benchmark`. The corresponding SXF lattice files are produced in `/home/oxygen/XML2ADXF` and `/home/oxygen/ADXF2SXF/`. The filenames are column headings in the following table.

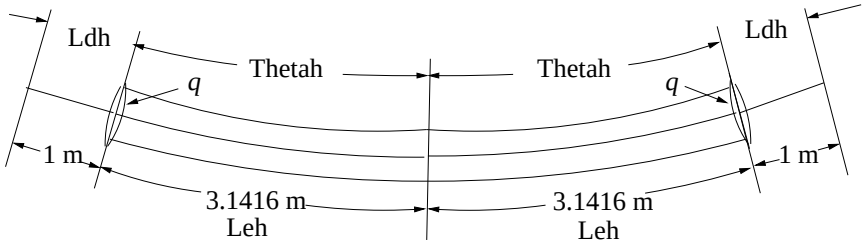

Figure 1: Single cell geometry. The full lattice consists of 40 identical cells.

Table 1: Parameters of benchmark all-electric EDM lattices, and Twiss parameters calculated from linearized transfer matrices. Note that the "half bend", and "half drift", elements are treated as individual elements in the sxf file. This gives 80 bends. The software treats these as 160 after slicing.

file name	variable name	unit	E_BM_M1.0.sxf	E_BM_Z.sxf	E_BM_P1.0.sxf
cells/arc	NCellPerArc		20	20	20
bend radius	r0	m	40.0	40.0	40.0
half drift length	Ldh	m	1.0	1.0	1.0
half bend per cell	Thetah	r	0.078539816	0.078539816	0.078539816
half bend length	Leh	m	3.141592	3.141592	3.141592
circumference	circum	m	331.327	331.327	331.327
inverse focal length	q	1/m	-0.002019	-0.00005960	0.0019075
field index	m		-1.0	1.0e-10	1.0
horizontal beta	betax	m	35.9237	36.1018	36.1910
vertical beta	betay	m	264.182	263.620	262.237
horizontal tune	Qx		1.4605	1.4578	1.4588
vertical tune	Qy		0.20024	0.20004	0.20047

3 Twiss Parameter Extraction

A once around transfer matrix at any point in the ring has the standard Twiss parameterization,

$$\mathbf{M} = \begin{pmatrix} \cos\mu + \alpha\sin\mu & \beta\sin\mu \\ -\frac{1+\alpha^2}{\beta}\sin\mu & \cos\mu - \alpha\sin\mu \end{pmatrix}. \tag{3}$$

At a mirror symmetry point in the lattice, α vanishes, though not in general. The phase advance $\mu = 2\pi Q$ can be obtained from

$$\cos\mu = \frac{M_{11} + M_{22}}{2}, \quad \text{and} \quad M_{12} = \beta\sin\mu. \tag{4}$$

β is, by definition, positive. These equations determine the signs of both $\cos\mu$ and $\sin\mu$. The four phase space quadrants, I/II/III/IV, are characterized by

cosine, sine sign pairs ++/-+/- -/+-. We then obtain the fractional parts of the phase advance from

$$\mu = \begin{cases} \cos^{-1}(\frac{M_{11}+M_{22}}{2}), & \text{if quadrant is I or II} \\ 2\pi - \cos^{-1}(\frac{M_{11}+M_{22}}{2}), & \text{if quadrant is III or IV} \end{cases}. \tag{5}$$

This still only partially resolves the aliasing ambiguity. Resolving the integer tune ambiguity requires keeping track of phase space quadrants while tracking through the lattice. This is described in captions to graphs below. We then obtain β from Eq. (4), and α from

$$\alpha = \frac{M_{11} - M_{22}}{2 \sin \mu}. \tag{6}$$

4 UAL/ETEAPOT Comparisons

For each of the three benchmark lattices, bunches of 21 standard particles are tracked for one turn. Each of the 80 bend elements is sliced in half for this analysis. The graphs show horizontal and vertical positions for two of the standard particles at the exits from each of the bends. The approximate tunes are calculated in the figure captions.

Once-around transfer matrices are obtained from the 21 standard particles using numerical differences. This differencing is based on the smallness (typically 1 micron spatial displacement, 1 microradian angular displacement) of the initial offsets. Sensitivity to these choices has not yet been investigated. Twiss parameters, β_x, β_y, and μ_x, μ_y are calculated using the procedure described above. The integer tunes (which this procedure does not provide) are obtained from the graphs. Values are given in the tables following the graphs.

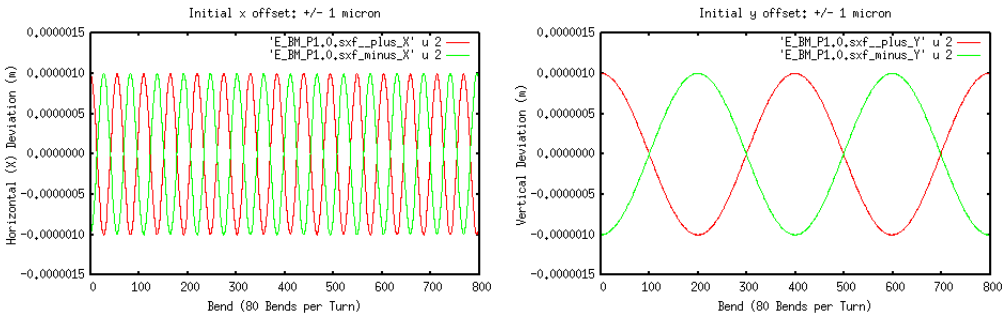

Figure 2: E_BM_P1.0.sxf: Horizontal Displacement: 10 turns, 1 sample per bend. $Q_x \approx 14.5$ osc/800 bends*80bends/turn=1.45 osc/turn. The integer part of the tune is $[Q_x] = 1$. Vertical Displacement: 10 turns, 1 sample per bend. $Q_y \approx 2.0$ osc/800 bends*80bends/turn=0.20 osc/turn. The integer part of the tune is $[Q_y] = 0$.

Table 2: E_TEAPOT comparisons for `E_BM_P1.0.sxf`.

file name	variable name	unit	linearized	2 slices/bend	
cells/arc	`NCellPerArc`		20		
bend radius	`r0`	m	40.0		
half drift length	`Ldh`	m	1.0		
half bend per cell	`Thetah`	r	0.078539816		
half bend length	`Leh`	m	3.141592		
circumference	`circum`	m	331.327		
inverse focal length	`q`	1/m	0.0019075		
field index	`m`		1.0		
horizontal beta	`betax`	m	36.1910	36.1910	
vertical beta	`betay`	m	262.237	262.2370	
horizontal tune	`Qx`		1.4588	1.4588	
vertical tune	`Qy`		0.20047	0.2005	

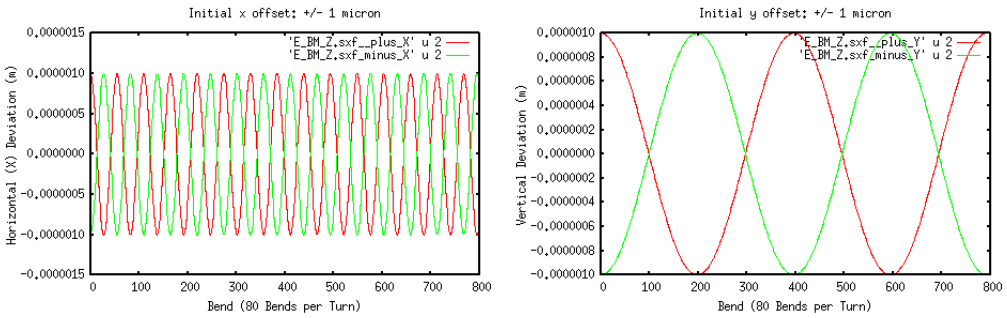

Figure 3: E_BM_Z.sxf: Horizontal Displacement: 10 turns, 1 sample per bend. $Q_x \approx 14.5$ osc/800 bends*80bends/turn=1.45 osc/turn. The integer part of the tune is $[Q_x] = 1$. Vertical Displacement: 10 turns, 1 sample per bend. $Q_y \approx$ 2.0 osc/800 bends*80bends/turn=0.20 osc/turn. The integer part of the tune is $[Q_y] = 0$.

Table 3: E_TEAPOTComparisons for `E_BM_Z.sxf`.

file name	variable name	unit	linearized	2 slices/bend	
cells/arc	`NCellPerArc`		20		
bend radius	`r0`	m	40.0		
half drift length	`Ldh`	m	1.0		
half bend per cell	`Thetah`	r	0.078539816		
half bend length	`Leh`	m	3.141592		
circumference	`circum`	m	331.327		
inverse focal length	`q`	1/m	-0.00005960		
field index	`m`		1.0e-10		
horizontal beta	`betax`	m	36.1018	36.0795	
vertical beta	`betay`	m	263.620	261.4688	
horizontal tune	`Qx`		1.4578	1.4581	
vertical tune	`Qy`		0.20004	0.2018	

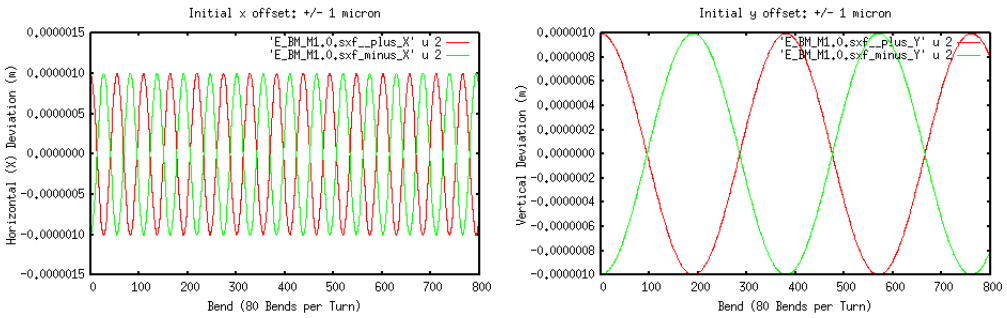

Figure 4: E_BM_M1.0.sxf: Horizontal Displacement: 10 turns, 1 sample per bend. $Q_x \approx 14.5$ osc/800 bends*80bends/turn=1.45 osc/turn. The integer part of the tune is $[Q_x] = 1$. Vertical Displacement: 10 turns, 1 sample per bend. $Q_y \approx 2.1$ osc/800 bends*80bends/turn=0.21 osc/turn. The integer part of the tune is $[Q_y] = 0$.

Table 4: E_TEAPOT comparisons for `E_BM_M1.0.sxf`

file name	variable name	unit	linearized	2 slices/bend	
cells/arc	`NCellPerArc`		20		
bend radius	`r0`	m	40.0		
half drift length	`Ldh`	m	1.0		
half bend per cell	`Thetah`	r	0.078539816		
half bend length	`Leh`	m	3.141592		
circumference	`circum`	m	331.327		
inverse focal length	`q`	1/m	-0.002019		
field index	`m`		-1.0		
horizontal beta	`betax`	m	35.9237	35.8566	
vertical beta	`betay`	m	264.182	251.8522	
horizontal tune	`Qx`		1.4605	1.4620	
vertical tune	`Qy`		0.20024	0.2102	

5 Comments and Conclusions

For the $m = 1$ case, there is exact agreement between the linearized analytic formulae and the tracking formalism. This is "as should be", but is far from automatic. The equations of the linearized transfer matrix formalism and the arbitrary-amplitude Munoz-Pavic seem utterly different. So the exact agreement confirms *both* approaches.

The agreement for $m \neq 1$ is excellent, but clearly not as good as $m = 1$. This strongly suggests that the kick compensation is not quite perfect. It is also not surprising that the deviation is proportional to $(m-1)^2$; for $m = 1$, the kick correction strength vanishes.

For most practical purposes, the code performance in the range $-1 \leq m \leq 1$ has been shown to be satisfactory. Nevertheless, minor further study seems to be justified. Two investigations seem natural. One is to vary the ($x_{\rm typ}$, $x'_{\rm typ}$, ...) parameters bigger and smaller by factors of, say, 10, to investigate this sensitivity. The other is to study the same 3 benchmark lattices with 4 slices per bend. (The code does not support 1 slice per bend).

References

[1] Storage Ring EDM Collaboration, *A Proposal to Measure the Proton Electric Dipole Moment with* 10^{-29} *e-cm Sensitivity,* especially Appendix 1. October, 2011

[2] C. Møller, *The Theory of Relativity,* Clarendon Press, Oxford, 1952,

[3] G. Muñoz and I. Pavic, *A Hamilton-like vector for the special-relativistic Coulomb problem,* Eur. J. Phys. **27**, 1007-1018, 2006

[4] R. Talman, *Geometric Mechanics,* John Wiley and Sons, 2000

[5] J. Aguirregabiria et al., Archiv:physics/0407049v1 [physics.ed-ph] 2004,

[6] U. Torkelsson, Eur. J. Phys., **19**, 459, 1998,

[7] T. Boyer, Am. J. Phys. **72** (8) 992, 2004